Pharm Res (2012) 29:1425–1434
DOI 10.1007/s11095-012-0688-6

RESEARCH PAPER

In Vitro and *In Vivo* Characterisation of PEG-Lipid-Based Micellar Complexes of Salmon Calcitonin for Pulmonary Delivery

Leonie Baginski • Oliviero L. Gobbo • Frederic Tewes • Johanna J. Salomon • Anne Marie Healy • Udo Bakowsky • Carsten Ehrhardt

Received: 19 August 2011 / Accepted: 17 January 2012 / Published online: 10 February 2012

ABSTRACT

Purpose To investigate DSPE-PEG_{2000}-based micellar formulations of salmon calcitonin (sCT) for their ability to improve pulmonary delivery.

Methods Micelles were characterised by DLS and ^{31}P-NMR spectroscopy. Stability against sCT degrading peptidases, trypsin, α-chymotrypsin and neutrophil elastase as well as their influence on transepithelial absorption was investigated *in vitro*. *In vivo* perfomance of sCT micelles was studied in an experimental model of intratracheal aerosolisation into rats.

Results Micelles with a mean hydrodynamic diameter of 12 nm spontaneously assembled, when a total concentration of 0.02 mM of PEG-lipid and sCT (at 1:1 molar ratio) was exceeded. Nuclear magnetic resonance confirmed the presence of small micellar structures. The micellar formulation showed increased stability against enzymatic digestion. *In vitro* studies also showed that sCT micelles were able to enhance transepithelial absorption. Data obtained from *in vivo* experiments provided evidence of significantly ($P < 0.05$) higher mean plasma concentrations of sCT, after inhalation of micelles compared to sCT solution, at 60 and 90 min, a significantly higher AUC_{inf} and a relative bioavailability of 160 ± 55% when compared to plain sCT solution.

Conclusions The herein described PEG-lipid micelles are promising carriers for enhanced pulmonary delivery of sCT.

L. Baginski • O. L. Gobbo • F. Tewes • J. J. Salomon • A. M. Healy • C. Ehrhardt (✉)
School of Pharmacy and Pharmaceutical Sciences
Trinity College Dublin
Dublin 2, Dublin, Ireland
e-mail: ehrhardc@tcd.ie

L. Baginski • U. Bakowsky
Department of Pharmaceutical Technology and Biopharmaceutics
Philipps University Marburg
Marburg, Germany

KEY WORDS bone disorders · DSPE-PEG · peptide delivery · pulmonary drug delivery · serine proteases

ABBREVIATIONS

CMC	critical micelle concentration
DLS	diffusion light scattering
DSPE-PEG	1,2-Distearoyl-*sn*-glycero-3-phosphoethanolamine-N-[methoxy(polyethylene glycol)-2000] ammonium salt
LDV	laser Doppler velocimetry
PdI	polydispersity Index
sCT	salmon calcitonin

INTRODUCTION

Salmon calcitonin (sCT), a 32-amino-acid peptide hormone that has been approved for the treatment of hypercalcaemia associated with malignent diseases and for the treatment of bone disorders such as osteoporosis and Paget's disease. It is currently marketed as injectable solutions (Calcimar®, Miacalcin®) as well as nasal sprays (Fortical®, Miacalcin®). Parenteral administration, however, is not very patient-friendly and the available nasal formulations show a wide window of bioavailability, ranging from 0.3 to 30% relative to injection (1). Such limitations as well as the drug's poor performance when given orally can potentially be avoided by pulmonary administration (2,3), as inhalation remains one of the most promising non-invasive route for systemic administration of macromolecules (4).

The withdrawal of Exubera® (the Pfizer/Nektar inhalable insulin) from the market, resulted in increased scepticism towards pulmonary macromolecule delivery. Afrezza®

(MannKind's insulin product), however, has started a new wave of interest in inhalable peptide drugs for systemic action, and it seems to have overcome some of the drawbacks that led to the failure of Exubera® (5). Compared to larger peptides like insulin, smaller compounds often suffer from unusually high enzymatic degradation in the lung (6–8). Nadkarni *et al.* (9), for example, demonstrated that peptide YY (PYY), an endogenous 36-amino acid peptide and food intake suppressant, showed a remarkable effect on the appetite of rats when administered via the pulmonary route. Nevertheless, the absolute bioavailability remained low, at 12–14%, suggesting a loss of the peptide within the lung by ways other than absorption (9). Considering the fact, that many catabolising peptidases are synthesised by lung epithelial cells and macrophages (10–12), it seems likely that PYY is degraded by proteolytic enzymes to a large extent, before it can reach the systemic circulation.

Structural modifications (e.g., by PEGylation) are an effective means to protect the peptide from proteolytic degradation (reviewed in (13,14)). Chemical attachment of PEG residues to polypeptides, however, can be accompanied by a decrease in the drug's bioactivity due to impeded receptor/ligand interactions as was observed for Pegasys®, Roche's PEGylated interferon α-2a (15). Different approaches to the conjugation of PEG (16–20) or PEG-lipids (21,22) to sCT have been reported in the literature. However, only Youn and co-workers focused their work on the pulmonary delivery of the peptide by synthesising three different Lys^{18}-PEGylated sCT derivatives, which strongly differed in regards to their hypocalcaemic efficacy and their ability to shield the peptide from proteolytic enzymes (23).

The rationale of this work was to develop a sCT formulation suitable for pulmonary application that takes advantage of the favourable shielding characteristics of the PEG residues, but at the same time, preserves the bioactivity of the peptide. In micelles, sCT is associated with but not chemically linked to amphiphilic molecules like PEG-lipids. Ideally, the micellar system will provide protection from enzyme degradation prior to absorption, while fully unfolding its therapeutic activity once it has reached the blood stream, resulting in enhanced bioavailability and maintained bioactivity.

MATERIALS AND METHODS

Materials

Calcitonin (salmon) Ph.Eur. (sCT; 3,432 Da) was purchased from Polypeptide Laboratories (Limhamn, Sweden), and 1,2-distearoyl-*sn*-glycero-3-phosphoethanolamine-N-[methoxy(polyethylene glycol)-2000] ammonium salt (DSPE-PEG; 2,804 Da) was purchased from Avanti Polar Lipids (INstruchemie BV, Delfzijl, Netherlands). Size and count rate were determined in Plastibrand disposable semi-micro-cuvettes (Brand, Wertheim, Germany) and ζ-potential in folded capillary cells (Zetasizer Nano series DTS 1060, Malvern Instruments, Herrenberg, Germany). For size, count rate and ζ-potential measurements, Aqua Ecotainer® (B. Braun, Melsungen, Germany) was used. Deuterium oxide (D_2O), phosphate buffered saline (PBS) tablets and neutrophil elastase were purchased from Sigma-Aldrich (Steinheim, Germany). Trypsin, treated with 1-chloro-3-tosylamido-4-phenyl-2-butanone and α-chymotrypsin, treated with 1-chloro-3-tosylamido-7-amino-2-heptanone were obtained from Worthington (Reading, United Kingdom). Acetonitrile, HPLC grade far UV, was purchased from Fisher Scientific (Dublin, Ireland), trifluoracetic acid (TFA) from Riedel-de Haën (Seelze, Germany). HPLC studies were performed on a LiChroCART®125-4 LiChrospher®100 RP-18 (5 µm) column (Merck, Darmstadt, Germany). For *in vivo* studies, Vetalar®, Domitor® and Antisedan® from Pfizer (Cork, Ireland) and SoloCath™ catheters from Linton Instrumentation (Diss, United Kingdom) were used. The salmon calcitonin ELISA kit S-1166 was purchased from Bachem (Weil am Rhein, Germany).

Preparation of Micelles and Physicochemical Characterisation

Salmon calcitonin was diluted in ultrapure water and the required amount of DSPE-PEG was added to the solution. Gentle agitation of the mixture assured homogenous distribution and formation of micelles.

The hydrodynamic diameter and polydispersity index (PdI) of the micelles was determined by dynamic light scattering (DLS) using a Zetasizer Nano ZS (Malvern Instruments) equipped with a 10 mW HeNe laser at a wavelength of 633 nm at 25°C. Scattered light was detected at an angle of 173°, the attenuator was manually adjusted to 11 and position to 4.65 mm for all measurements. For data analysis, the viscosity and refractive index of water were used. Values given are the mean ± standard deviation of at least 5 independent samples of which each was measured 3 times with 10 runs. The ζ-potential was measured with the same instrument at 25°C and a scattering angle of 17° by measuring the electrophoretic mobility by laser Doppler velocimetry (LDV). Samples contained 10^{-3} M sodium chloride and the pH was 7.4. Each sample was measured 3 times with 100 runs. Values given are the mean ± standard deviation.

Determination of the Aggregation Number of Polymer Molecules within One Micelle

According to Vorobyova and colleagues (24), the aggregation number p—expressed as the number of polymer molecules within a micelle—can be calculated using Eq. (1)

$$p = \frac{10\pi R_H^3 N_A}{3M[\eta]} \quad (1)$$

where R_H is the hydrodynamic radius, N_A is Avogadro's number, M is the molecular weight of the polymer, and η is the intrinsic viscosity.

Nuclear Magnetic Resonance (^{31}P-NMR)

^{31}P-NMR measurements were carried out as described by Leal *et al.* (25). Samples of DSPE-PEG sCT micelles (equimolar amounts) were prepared and measured in D_2O with 50 ppm spectral width at a resonance frequency of 202.47 MHz (11.7 T) on a JEOL ECA-500 spectrometer (JEOL, Eching, Germany) using a JEOL broadband observe probe (NM-03520TH5). One thousand scans were accumulated using 4.5 μs pulses. Prior to Fourier transformation, a line broadening of 30 Hz was applied. All measurements were performed at room temperature (25°C) and at 37°C.

Determination of the Critical Micelle Concentration (CMC)

The CMC of an equimolar mixture of sCT / DSPE-PEG in water was determined by DLS measuring the intensity of scattered light (in kilo counts per second). For DLS measurements the same instrument with identical setting was used as described above. Samples of the sCT / PEG-lipid mixtures in water with total concentrations of 0.006, 0.009, 0.012, 0.018, 0.024, 0.036, 0.048, 0.072 and 0.14 mM were analysed in disposable semi-micro-cuvettes. Values given are the mean ± standard deviation of 5 independent experiments with each experiment comprising 3 measurements of the same sample with 10 runs.

Stability against Trypsin, Chymotrypsin and Neutrophil Elastase Digestion

The digestion of plain sCT and DSPE-PEG sCT micelles by three sCT degrading enzymes, trypsin, chymotrypsin and neutrophil elastase was investigated according to a method modified from Marschütz and Bernkop-Schnürch (26). Micelles were prepared in water as described above with PEG-lipid and sCT at equal molarities. A trypsin solution containing 2 BAEE units trypsin per ml PBS (pH 7.4) and a chymotrypsin solution containing 0.2 TAME units chymotrypsin per ml PBS (pH 7.4) were prepared. Five-hundred microlitres of trypsin or chymotrypsin solution were added to the same volume of either plain sCT solution or the micellar complexes. In the case of neutrophil elastase, 500 μl PBS (pH 7.4) and 500 μl of either sCT solution or sCT-containing micelles were directly added to the 1-unit-vials of elastase. All samples containing 1 mg sCT (unmodified or in micelles) and 1 unit trypsin, 0.1 unit chymotrypsin or 1 unit neutrophil elastase, respectively, per ml solution were incubated at 37°C for 2 h. After 0, 10, 30, 60 and 120 min, samples of 180 μl were withdrawn, immediately diluted with an equal volume of 1% TFA and analysed by HPLC according to the method described below. Data are shown as mean ± standard deviation of 3 independent experiments.

High-Performance Liquid Chromatography (HPLC)

The instrument for reverse phase HPLC analyses consisted of a Shimadzu LC-1OAT VP pump, FCV-10AL VP low pressure gradient valve, DGU-14A degasser, SIL-10 AD VP autosampler, SPD-10A VP UV–VIS-detector and CLASS-VP software (Kyoto, Japan). Samples were analysed for their sCT content according to a method described by Shah and Khan (27) with modifications. In brief, the mobile phases consisted of 0.1% v/v TFA-water (A) and 0.1% v/v TFA-acetonitrile (B). A linear gradient was run at a flow-rate of 1 ml/min: 20–35% B for 10 min, 35–37% B from 10 to 20 min and 37–20% from 20 to 25 min. Twenty microlitres of sample were injected and analysed at a wavelength of 215 nm. Each sCT concentration was quantified from the corresponding integrated peak area.

Transepithelial Transport Experiments

In order to assess, if sCT and/or micellar complexes compromise the epithelial barrier, or if they indeed enhance absorption, transport experiments were carried out across confluent monolayers of Calu-3 cells. Transwell filter-grown cell monolayers were washed with warm Krebs-Ringer buffer (150 mM NaCl, 5.2 mM KCl, 2.2 mM $CaCl_2$, 0.2 mM $MgCl_2 \cdot 6H_2O$, 6 mM $NaHCO_3$, 5 mM HEPES, 2.8 mM glucose, pH 7.4) and equilibrated in the buffer for approximately 1 h. The buffer in the apical donor side was then replaced with a solution containing fluorescein sodium (FluNa; 50 μmol) alone or FluNa together with either sCT (10 μg/ml) or sCT and PEG-lipid (10 μg/ml each). The apical fluid volume was 520 μl and the initial concentration in the donor fluid was assayed by drawing a 20-μl sample, immediately after the initiation of transport studies. Two hundred microlitre samples were drawn serially from the receiver compartment at 15, 30, 45, 60 and 90 min. After each sampling, fresh transport

buffer of an equal volume was returned to the receiver side to maintain a constant volume. At the end of the transport experiment, a 20-µl sample was drawn from the donor fluid and assayed for its activity. Each experiment was performed employing a total of 4 cell layers. In order to assess the integrity of monolayers during the transport studies, transepithelial electricl resistance (TEER) was measured before and after the experiment.

Flux (J) was determined from steady-state appearance rates of FluNa in the receiver fluid. The apparent permeability coefficient, P_{app}, was calculated according to Eq. (2)

$$P_{app} = J/(A \cdot C_i) \tag{2}$$

where C_i was the initial concentration of the drug under investigation in the donor fluid and A the nominal surface area of cell layers (1.13 cm^2) utilised in this study. Fluorescence of samples was analysed in 96-well plates using a fluorescence plate reader (FLUOstar Optima, BMG Labtech, Offenburg, Germany) at excitation and emission wavelengths of 485 and 520 nm, respectively. The samples were diluted with KRB, where appropriate.

In Vivo Experiments

Animals

The experimental protocols employed in this study were approved by the Animal Research Ethics Committee, Trinity College Dublin (TCD) and the Department of Health and Children (Ireland), in accordance with the European Community Directive (86/609). The animals used for experiments were male Wistar rats supplied by the TCD BioResources Unit, with a body weight of 350±50 g. The animals were housed in a thermo-regulated environment with a 12-h light/dark cycle. Food and water were available *ad libitum*.

Surgery

Rats were anaesthetised by an intraperitoneal injection with a mixture of ketamine hydrochloride (Vetalar®) and medetomidine hydrochloride (Domitor®), before a heparinised catheter (SoloCath™) was installed into the left femoral artery for blood sampling. The left femoral vein was cannulated for the administration of sCT solution.

Drug Administration

The sCT dose for intratracheal administration of plain solution and PEG-lipid micelles was 100 µg/kg in 100 µl KRB. The aerosolisation was performed using an AeroProbe™ intracorporeal nebulising catheter controlled by a LabNeb™ unit (Trudell Medical International, London, ON, Canada) according to the manufacturer's protocol. The intravenous bolus administration of sCT (also at 100 µg/kg) was performed by injecting 500 µl of sCT solution in KRB.

Blood Sampling

After drug administration, the sedation was reversed by injection of atipamezole hydrochloride (Antisedan®) and blood sampling was carried out from freely moving animals. Arterial blood samples (200 µl) were serially collected in heparinised tubes 0, 3, 10, 20, 30, 60, 90, 120 and 180 min post sCT administration. Blood samples were centrifuged at 10,000 rcf for 5 min, before plasma was collected and stored at −20°C until further use.

Calcitonin Measurement

Samples were assayed using a high-sensitive sCT ELISA kit according to the manufacturer's protocol.

Pharmacokinetic Analysis

Pharmacokinetic parameters were determined for each individual rat using a two-compartment model. Salmon calcitonin plasma concentration (C_p) *versus* time profiles were best fitted with Eq. (3) using the least-squares method and the solver function of the Excel® software, 2007 (Microsoft, USA).

$$C_p = A \cdot e^{-\alpha \cdot t} + B \cdot e^{-\beta \cdot t} + C \cdot e^{-ka \cdot t} \tag{3}$$

with $\alpha > \beta$, and C=0 for profiles fitting after *i.v.* administration, and C=−(A + B) for profiles fitting after pulmonary administration. In this equation, the *A, B,* α and β terms were functions of the rate constant *k12, k21, kel* according to Eqs. (4), (5) and (6).

$$kel = \frac{\alpha \cdot \beta}{k21} \tag{4}$$

$$k12 = \alpha + \beta - k21 - kel \tag{5}$$

$$k21 = \frac{\alpha \cdot B + A \cdot \beta}{A + B} \tag{6}$$

Area under plasma concentration-*versus*-time profiles *(AUC)* was calculated by using the linear trapezoidal rule. To determine the AUC infinity (AUC_{inf}), the area remaining after the last measured concentration ($C_{t\to\infty}$) was extrapolated using Eq. (7).

$$AUC_{t\to\infty} = \frac{C_{t\to\infty}}{\beta} \tag{7}$$

The absolute bioavailability (F_{abs}) was calculated by comparison of the sCT AUC_{inf} obtained after intratracheal

(i.t.) administration to the one obtained by *i.v.* at the same dose as in Eq. (8).

$$F_{abs} = \frac{AUC_{\text{inf } i.t.}}{AUC_{\text{inf } i.v.}} \quad (8)$$

The relative bioavailability (F_{rel}) was calculated by comparing the AUC_{inf} of *i.t.* administered micellar formulation with the AUC_{inf} of the same dose of *i.t.* administered sCT solution using Eq. (9).

$$F_{rel} = \frac{AUC_{\text{inf micelle}}}{AUC_{\text{inf sCT}}} \quad (9)$$

Statistical Data Analysis

Data were analysed by F-test and *t*-test. Values were considered statistically significant when $P<0.05$.

RESULTS

Physicochemical Characterisation of Micelles

Micelles with different molar ratios of PEG-lipid and sCT (i.e., 4:1, 2:1, 1:1 and 1:2) were prepared and analysed by SEC and DLS. At all investigated ratios, micelles with comparable diameters of 12–13 nm were formed. In addition, this size range was confirmed by cryo-TEM pictures (data not shown). The lowest DSPE-PEG:sCT molar ratio at which sCT was completely incorporated in the micelle was 1:1. At this ratio, only a single peak was detected in SEC analyses, whereas higher amounts of sCT resulted in a second peak with longer retention time in the SEC spectrum due to unbound sCT (data not shown). The 1:1 ratio can hence be considered the saturation ratio of sCT to PEG-lipid, and was chosen for further investigations. Whilst solutions of pure sCT (0.6 mM) or DSPE-PEG (0.6 mM) in water both showed particle sizes≤ 2 nm, spontaneous self-assembly of micelles with a mean hydrodynamic diameter of 12 nm was observed, when the two compounds were added at a 1:1 ratio (each 0.6 mM) in water. A PdI of 0.15±0.04 was obtained for these systems and a ζ-potential of 1.54±0.20 mV was measured.

Determination of the Aggregation Number of Polymer Molecules within One Micelle

We used the method described by Vorobyova *et al.* (24) to determine the number of polymer molecules in a micelle. In this work, micelles are not formed of a single compound, but of a 1:1 ratio of sCT and DSPE-PEG. Thus, a molecular weight equal to sCT + DSPE-PEG (6,235 g/mol) and an intrinsic viscosity of 0.1 dl/g (0.09 for PEG 2000) were used for the estimation of the aggregation number. For a hydrodynamic diameter of 12 nm—as it was determined by DLS measurements—the aggregation number was approximately 22. One micelle was therefore composed of about 22 sCT molecules and 22 DSPE-PEG molecules.

^{31}P-NMR Spectroscopy

Peak formation in ^{31}P-NMR spectra can be used to distinguish between micellar and liposomal formulations (25). The ^{31}P-NMR signal depends on the molecular order of phospholipids in the particle into which the molecule is embedded. Small micellar particles show symmetric narrow sharp peaklines compared to wider peaks of liposomes with their bigger entity (25,28). ^{31}P-NMR spectra of the DSPE-PEG sCT mixture (Fig. 1) showed symmetric sharp peaks and therefore, confirmed the presence of small micellar structures at room temperature (i.e., 25°C), as well as at body temperature (i.e., 37°C).

Determination of the Critical Micelle Concentration (CMC)

A plot comparing the intensity of scattered light and the mean hydrodynamic diameter obtained for various concentrations of sCT and DSPE-PEG (at a 1:1 ratio) is illustrated in Fig. 2. The intersection of the two regression lines of the intensity data (i.e., the CMC) was calculated to be 0.02 mM (i.e., 0.01 mM sCT plus 0.01 mM DSPE-PEG in water). At lower concentrations, where surfactant molecules are non-associated monomers (29), no reliable size distribution information could be obtained and the autocorrelation functions showed very low intercepts. Once the CMC was reached, however, the scattering intensity showed a linear increase with concentration, and particle sizes of 12–14 nm (depending on the concentration) were measured and autocorrelation functions showed much higher intercepts.

Stability against Trypsin, Chymotrypsin and Neutrophil Elastase Digestion

A protective effect of the DSPE-PEG sCT micelles against enzymatic degradation was observed, when compared to plain sCT. The degradation profiles of the three different enzymes are illustrated in Fig. 3. When incubated with trypsin, degradation of sCT micelles and plain sCT showed a small, albeit significant ($P<0.05$) advantage for the micellar formulations after 120 min, with the sCT content of micelles being reduced to 39.02±0.88% of the original concentration, compared to 36.60±1.01% in the case of plain sCT. Chymotrypsin reduced sCT to 56.29±0.96% in the micelles after 120 min, which was significantly ($P<0.05$) higher than the 45.89±3.19% remaining for plain sCT. Neutrophil elastase dramatically reduced micellar sCT to 27.18±8.06% of the

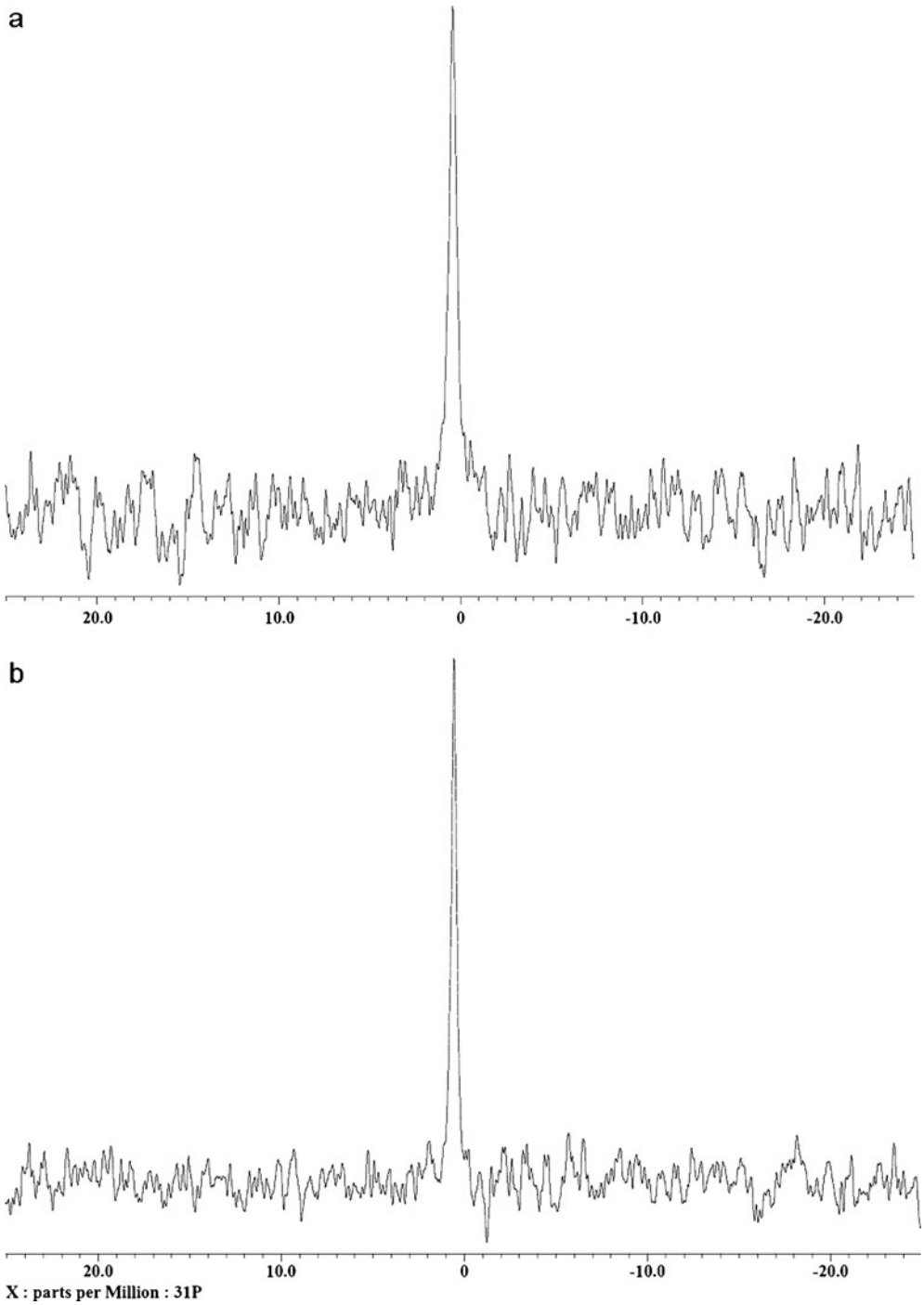

Fig. 1 ^{31}P-NMR spectra of DSPE-PEG sCT micelles at 25°C (**a**) and 37°C (**b**). Narrow symmetric peaks indicate the presence of small micellar structures at both temperatures.

original concentration, whereas 8.80±11.48% of plain sCT was left after 120 min. This difference, however, was not significant ($P>0.05$). Figure 4 summarises the stability data of incubation with the three different enzymes after 120 min.

Effect of sCT and sCT Micelles on Transepithelial Absorption

Transport studies with the paracellular marker compound, fluorescein sodium, revealed no differences in absorptive flux, when sCT was included in the donor compartment (Fig. 5). Addition of PEG-lipid, and hence formation of micellar sCT complexes, resulted in a significant ($P>0.05$) increase in FluNa absorption. Interestingly, this increase in P_{app} was not accompanied by a decrease in TEER (data not shown).

In Vivo Experiments

The individual plasma concentration *vs.* time profiles of intratracheally administered sCT micelles are shown in Fig. 6.

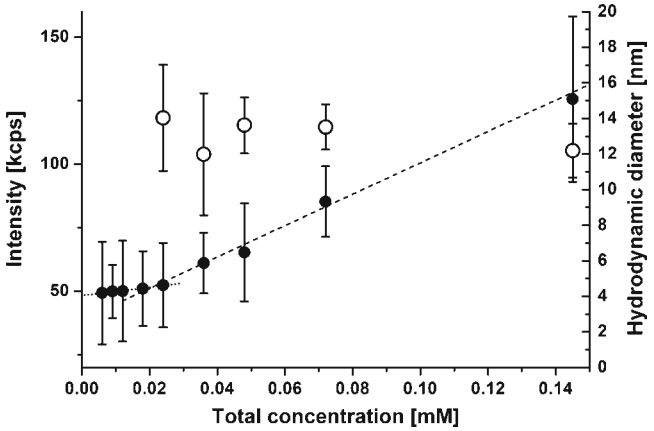

Fig. 2 The intensity of scattered light (*filled circle*) and the mean hydrodynamic diameter (*empty circle*) obtained for different concentrations of sCT and DSPE-PEG (at equimolar amounts). The intersection of the two regression lines of the intensity data (i.e., the CMC) was calculated to be 0.02 mM. Values are given as means ± SD; $n=5$.

When compared to free sCT in solution, PEG-lipid micelles resulted in higher mean plasma concentrations at all time points, which were significantly different ($P<0.05$) at 60 and 90 min (Fig. 7). The maximum plasma concentration (c_{max}) and the time at which it was reached (t_{max}) were both slightly increased for the micellar formulation compared to *i.t.* administered sCT solution. Table I summarises the pharmacokinetic parameters, AUC_{inf}, F_{abs}, F_{rel}, c_{max} and t_{max}. The AUC_{inf} for sCT micellar complexes was 23±8 min·ng/ml/µg·kg, and therefore significantly ($P<0.05$) higher that the AUC_{inf} for free sCT which was determined as 14±6 min·ng/ml/µg·kg. Relative and absolute bioavailabilities were hence, both significantly ($P<0.05$) increased by more than 60% (Table I).

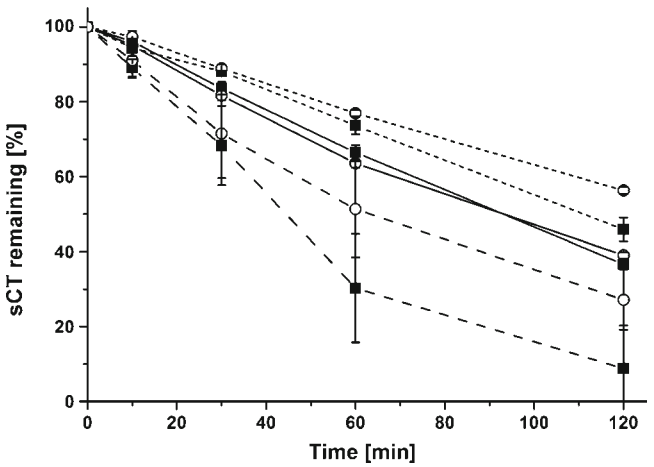

Fig. 3 Stability of plain sCT (*filled square*) compared to sCT assembled into DSPE-PEG micelles (*empty circle*) in the presence of 1 unit trypsin (*solid line*), 0.1 unit α-chymotrypsin (*dotted line*) or 1 unit neutrophil elastase (*dashed line*), respectively. Samples were withdrawn after 0, 10, 30, 60 and 120 min of incubation at 37°C and analysed by HPLC. Peak areas were used to determine the sCT concentrations, here shown as the amount of sCT remaining [%] over time. Data are represented as mean ± SD; $n=3$.

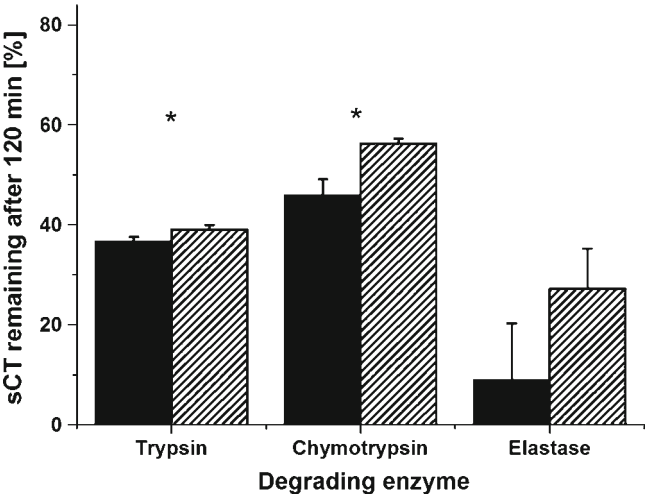

Fig. 4 Protection of free sCT (*black bars*) and micellar complexes (*shaded bars*) against enzymatic digestion. The peptide was incubated in the presence of trypsin, α-chymotrypsin or neutrophil elastase for 120 min at 37°C, before samples were analysed by HPLC. The amount of sCT remaining [%] of the original concentration is represented as means ± SD; $n=3$; * $P<0.05$.

DISCUSSION

This work set out to determine if micellar complexes could result in an improvement in the pulmonary delivery of salmon calcitonin. Micelles prepared from sCT and DSPE-PEG_{2000} were characterised by DLS, LDV and ^{31}P-NMR. *In vitro*, the micellar sCT formulation proved to be more stable against degradation by trypsin, chymotrypsin and neutrophil elastase than plain sCT. *In vivo* experiments showed that plasma concentrations were significantly higher post micellar administration than after aerosolisation of sCT solution after 60 and 90 min and that the bioavailability

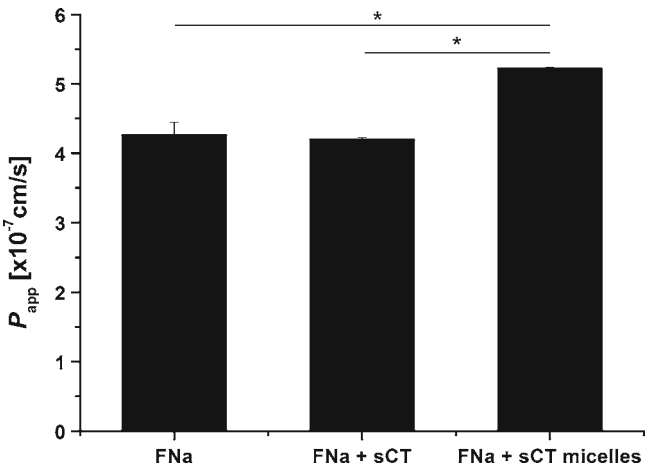

Fig. 5 Effect of sCT and micellar complexes on transport of fluorescein sodium *in vitro*. Permeability of FluNa was measured across Calu-3 respiratory epithelial cell monolayers alone, and in the presence of either sCT or sCT DSPE-PEG micelles. Whilst sCT had no influence on FluNa P_{app}, micellar complexes significantly increased its absorption. Data are represented as mean ± SD; $n=4$; * $P<0.05$.

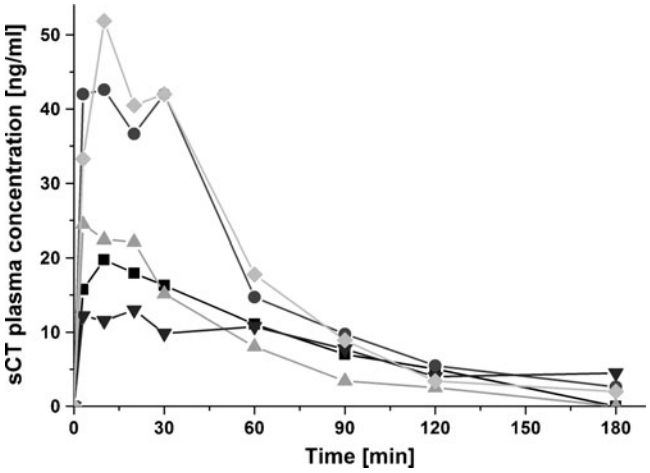

Fig. 6 Plasma concentrations of intratracheally aerosolised micellar complexes of sCT (100 μg/kg). The graphs show the individual plasma concentrations (ng/ml) of five investigated rats.

(absolute and relative) of the micellar formulation was significantly ($P<0.05$) increased compared to the sCT solution. However, the effect observed *in vivo* was more pronounced than the increase in stability *in vitro* would suggest. Results from *in vitro* transport study further supported the notion that the shielding from catabolising peptidases may be accompanied by a permeability enhancing effect of the formulation.

After intratracheal instillation of sCT *in vivo*, an absolute bioavailability of 17% was measured by Patton *et al.* in rat lungs (30), and Clark *et al.* (31) reported relative bioavailabilities of 10-18% for nebulised sCT solution compared to *s.c.* injection in healthy volunteers. It is, however, desirable to further increase the efficiency of peptide delivery, in order to reduce local side effects, and also the costs associated with the therapy. In previous studies we showed that peptidases and proteinases play a significant role in the pulmonary breakdown of sCT (32)

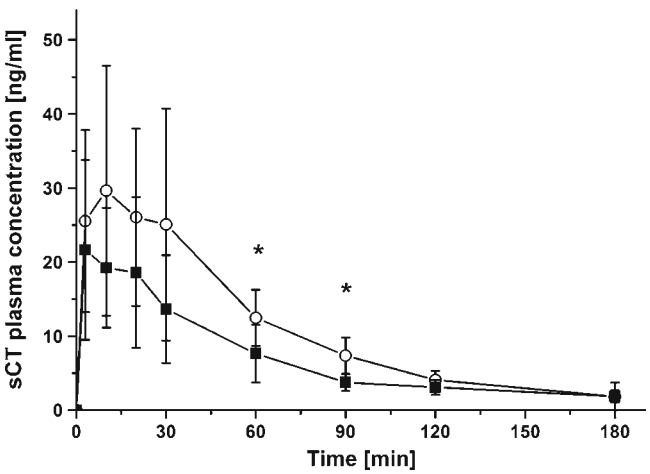

Fig. 7 Plasma concentrations of intratracheally aerosolised sCT solution (*black square*) ($n=7$) and DSPE-PEG micelles (*empty circle*) e$n=5$), both given at a concentration of 100 μg/kg. Data is represented as mean ± SD; * $P<0.05$.

Table I Pharmacokinetic Parameters of Intratracheally Aerosolised and Injected sCT (100 μg /kg) and PEG-Lipid sCT Micelles ($n=5$–7)

	sCT solution (*i.v.*)	sCT solution (*i.t.*)	DSPE-PEG micelles (*i.t.*)
AUC_{inf} [min*ng/ml/μg*kg]	125 ± 35	14 ± 6	23 ± 8
F_{abs} [%]	100 ± 28	11 ± 5	18 ± 6
F_{rel} [%]		100 ± 39	160 ± 55
c_{max} [ng/ml]	489 ± 48	22 ± 12	30 ± 17
t_{max} [min]		5 ± 4	7 ± 4

and therefore formulations that protect from proteolytic degradation are a key element of improving macromolecule delivery via the lungs. Several groups have demonstrated that direct conjugation of sCT with PEG alone or PEG and lipids can enhance the peptide's stability against digestion by proteases (16–23). Direct PEGylation, however, generally comes at the cost of significantly reduced bioactivity (14,15,23). Our aim was, therefore, to develop a more transient delivery approach based on PEG-lipid-peptide self assembly.

The amphiphilic properties of the α-helical salmon calcitonin have previously been reported and it was suggested that the hydrophobic residues of the molecule face to one side of the helix, while the hydrophilic amino acids orient to the other (33–35). It therefore is likely, that DSPE-PEG associates with sCT in such a way that the PEG-groups loosely interact with the hydrophilic components of the sCT molecules and together form the outer part of the micelle, whereas the lipid-chain and lipophilic residues of sCT are stowed in the interior of the micelle. Moreover, it was reported several years ago that proteins are able to bind equimolar amounts of amphiphilic tensides, and that this binding was caused by hydrophobic interactions (36). Reynolds and Tanford (36) also emphasised that the protein was not incorporated in the interior of a micelle nor interacted with the surface of tenside micelles, but that the tenside monomers interacted with the macromolecule and together formed micelle-like structures.

To our knowledge, this is the first report on micellar systems comprising a peptide drug and a PEG-lipid being tested for pulmonary application with the aim of achieving a systemic action. Cheng and Lim observed the assembly of PEG-lipid sCT conjugates in water into larger particles (21,22). Conjugates with a fatty acid molecule and one or two separate PEG_{5000}-chains, associated to particles with radii of 34±17 nm and 68±21 nm, respectively (21). Conjugates of sCT and a PEG_{5000}-lipid molecule resulted in complexes with a radius of 30±9 nm (22). However, our data suggest that not only conjugates, but also mixtures of the non-conjugated compounds (i.e., PEG-lipid and sCT) result in association into micelles, and that these systems are suitable carriers for peptide drugs. Similar observations have recently been published by Castelletto *et al.* (37), Kastantin *et al.* (38) and Lim *et al.* (39).

Castelletto *et al.* (37) and Kastantin *et al.* (38) thoroughly investigated the interaction of bovine serum albumin (BSA) with DSPE-PEG_{2000} micelles and found that BSA possesses binding sites for the adsorption of PEG-lipid monomers leading to the formation PEG-lipid protein complexes. Lim *et al.* (39) observed that DSPE-PEG_{2000} self-associated spontaneously with the 30-amino acid peptide, glucagon-like peptide 1 (GLP-1). After subcutaneous injection, the micellar GLP-1 showed promising anti-inflammatory properties in the treatment of acute lung injury. With a diameter of 14 ± 3 nm the GLP-1 micelles were of comparable size to the sCT micelles of this study. Lim *et al.* prepared DSPE-PEG-micelles first and subsequently added the peptide and found a lipid:peptide saturation molar ratio of 13:1 (39), whereas our data indicates a lipid:peptide saturation molar ratio of 1:1. The differences in preparation might explain the observation of Lim and co-workers that some GLP-1 molecules spontaneously associate to the DSPE-PEG micelles (39,40), whereas our results support the hypothesis of Reynolds and Tanford (36) that the peptide interacts with the tenside monomers to form micellar structures, but that the sCT is not incorporated into micelles formed solely of tenside.

CONCLUSIONS

Micelles of a 1:1 ratio of DSPE-PEG and sCT showed increased stability against catabolic enzymes, enhanced transepithelial absorption and thus, resulted in an enhanced pharmacokinetic performance *in vivo*. Ongoing studies will focus on the short- and long-term toxicity of the system, as well as on immunogenicity concerns and stability aspects during storage and release. These are important considerations that might turn into roadblocks if not identified early enough (41).

ACKNOWLEDGMENTS & DISCLOSURES

The authors acknowledge funding by a Strategic Research Cluster grant (07/SRC/B1154) under the National Development Plan co-funded by EU Structural Funds and Science Foundation Ireland. The authors thank Dr. Thomas Kämpchen (Philipps University Marburg) for performing the ^{31}P-NMR studies, Felix Gut (Philipps University Marburg) for the creation of sCT—DSPE-PEG molecule model, and the group of Prof. Dr. Thomas Kissel (Philipps University Marburg) for technical support.

REFERENCES

1. Stevenson CL. Advances in peptide pharmaceuticals. Curr Pharm Biotechnol. 2009;10(1):122–37.
2. Patton JS. Mechanisms of macromolecule absorption by the lungs. AdvDrug Deliv Rev. 1996;19(1):3–36.
3. Siekmeier R, Scheuch G. Systemic treatment by inhalation of macromolecules–principles, problems, and examples. J Physiol Pharmacol. 2008;59(6):53–79.
4. Patton JS, Brain JD, Davies LA, Fiegel J, Gumbleton M, Kim KJ, *et al.* The particle has landed–characterizing the fate of inhaled pharmaceuticals. J Aerosol Med Pulm Drug Deliv. 2010;23(2): S71–87.
5. Neumiller JJ, Campbell RK. Technosphere insulin: an inhaled prandial insulin product. BioDrugs. 2010;24(3):165–72.
6. Adjei LA, Carrigan PJ. Pulmonary bioavailability of LH-RH analogs: some pharmaceutical guidelines. J Biopharm Sci. 1992;3: 247–54.
7. Patton JS, Nagarajan S, Clark A. Pulmonary absorption and metabolsim of peptides and proteins. Respiratory Drug Delivery VI. 1998;1:17–24.
8. Patton J, Byron P. Inhaling medicines: delivering drugs to the body through the lungs. Nat Rev Drug Discov. 2007;6(1):67–74.
9. Nadkarni PP, Costanzo RM, Sakagami M. Pulmonary delivery of peptide yy for food intake suppression and reduced body weight gain in rats. Diabetes Obes Metab. 2011;13:408–17. doi:10.1111/j.1463-1326.2011.01363.x.
10. Wall DA. Pulmonary absorption of peptides and proteins. Drug Delivery. 1995;2:1–20.
11. Hussain A, Arnold JJ, Khan MA, Ahsan F. Absorption enhancers in pulmonary protein delivery. J Control Release. 2004;94(1):15–24.
12. Baginski L, Tachon G, Falson F, Patton JS, Bakowsky U, Ehrhardt C. Reverse transcription polymerase chain reaction (RT-PCR) analysis of proteolytic enzymes in cultures of human respiratory epithelial cells. J Aerosol Med Pulm Drug Deliv. 2011;24(2):89–101.
13. Veronese FM, Pasut G. PEGylation, successful approach to drug delivery. Drug Discov Today. 2005;10(21):1451–8.
14. Harris JM, Chess RB. Effect of pegylation on pharmaceuticals. Nat Rev Drug Discov. 2003;2(3):214–21.
15. Bailon P, Palleroni A, Schaffer CA, Spence CL, Fung WJ, Porter JE, *et al.* Rational design of a potent, long-lasting form of interferon: a 40 kDa branched polyethylene glycol-conjugated interferon alpha-2a for the treatment of hepatitis C. Bioconjug Chem. 2001; 12(2):195–202.
16. Na DH, Youn YS, Park EJ, Lee JM, Cho OR, Lee KR, *et al.* Stability of PEGylated salmon calcitonin in nasal mucosa. J Pharm Sci. 2004;93(2):256–61.
17. Lee KC, Moon SC, Park MO, Lee JT, Na DH, Yoo SD, *et al.* Isolation, characterization, and stability of positional isomers of mono-PEGylated salmon calcitonins. Pharm Res. 1999;16(6):813–8.
18. Shin BS, Jung JH, Lee KC, Yoo SD. Nasal absorption and pharmacokinetic disposition of salmon calcitonin modified with low molecular weight polyethylene glycol. Chem Pharm Bull (Tokyo). 2004;52(8):957–60.
19. Youn Y, Jung J, Oh S, Yoo S, Lee K. Improved intestinal delivery of salmon calcitonin by Lys18-amine specific PEGylation: stability, permeability, pharmacokinetic behavior and *in vivo* hypocalcemic efficacy. J Control Release. 2006;114(3):334–42.
20. Youn YS, Na DH, Lee KC. High-yield production of biologically active mono-PEGylated salmon calcitonin by site-specific PEGylation. J Control Release. 2007;117(3):371–9.
21. Cheng W, Lim LY. Synthesis, characterization and *in vivo* activity of salmon calcitonin coconjugated with lipid and polyethylene glycol. J Pharm Sci. 2009;98(4):1438–51.
22. Cheng W, Lim LY. Design, synthesis, characterization and *in-vivo* activity of a novel salmon calcitonin conjugate containing a novel PEG-lipid moiety. J Pharm Pharmacol. 2010;62(3):296–304.
23. Youn YS, Kwon MJ, Na DH, Chae SY, Lee S, Lee KC. Improved intrapulmonary delivery of site-specific PEGylated salmon

calcitonin: optimization by PEG size selection. J Control Release. 2008;125(1):68–75.
24. Vorobyova O, Lau W, Winnik MA. Aggregation number determination in aqueous solutions of a hydrophobically modified poly (ethylene oxide) by fluorescence probe techniques. Langmuir. 2001;17:1357–66.
25. Leal C, Rögnvaldsson S, Fossheim S, Nilssen EA, Topgaard D. Dynamic and structural aspects of PEGylated liposomes monitored by NMR. J Colloid Interface Sci. 2008;325(2):485–93.
26. Marschütz MK, Bernkop-Schnürch A. Oral peptide drug delivery: polymer-inhibitor conjugates protecting insulin from enzymatic degradation *in vitro*. Biomaterials. 2000;21(14):1499–507.
27. Shah R, Khan M. Protection of salmon calcitonin breakdown with serine proteases by various ovomucoid species for oral drug delivery. J Pharm Sci. 2004;93(2):392–406.
28. Cullis PR, De Kruijff B. Polymorphic phase behaviour of lipid mixtures as detected by 31P NMR. Evidence that cholesterol may destabilize bilayer structure in membrane systems containing phosphatidylethanolamine. Biochim Biophys Acta. 1978;507(2):207–18.
29. Helenius A, McCaslin DR, Fries E, Tanford C. Properties of detergents. Methods Enzymol. 1979;56:734–49.
30. Patton JS, Trinchero P, Platz RM. Bioavailability of pulmonary delivered peptides and proteins: [alpha]-interferon, calcitonins and parathyroid hormones. J Control Release. 1994;28(1–3):79–85.
31. Clark A, Kuo MC, Newman S, Hirst P, Pitcairn G, Pickford M. A comparison of the pulmonary bioavailability of powder and liquid aerosol formulations of salmon calcitonin. Pharm Res. 2008;25 (7):1583–90.
32. Baginski L, Tewes F, Buckley ST, Healy AM, Bakowsky U, Ehrhardt C. Investigations into the Fate of Inhaled Salmon Calcitonin at the Respiratory Epithelial Barrier. Pharm Res. 2012;29(1):332–41.
33. Kaiser ET, Kézdy FJ. Amphiphilic secondary structure: design of peptide hormones. Science. 1984;223(4633):249–55.
34. Moe GR, Kaiser ET. Design, synthesis, and characterization of a model peptide having potent calcitonin-like biological activity: implications for calcitonin structure/activity. Biochemistry. 1985; 24(8):1971–6.
35. Andreotti G, Méndez BL, Amodeo P, Morelli MA, Nakamuta H, Motta A. Structural determinants of salmon calcitonin bioactivity: the role of the Leu-based amphipathic alpha-helix. J Biol Chem. 2006;281(34):24193–203.
36. Reynolds JA, Tanford C. Binding of dodecyl sulfate to proteins at high binding ratios. Possible implications for the state of proteins in biological membranes. Proc Natl Acad Sci U S A. 1970;66(3):1002–7.
37. Castelletto V, Krysmann M, Kelarakis A, Jauregi P. Complex formation of bovine serum albumin with a poly(ethylene glycol) lipid conjugate. Biomacromolecules. 2007;8(7):2244–9.
38. Kastantin M, Missirlis D, Black M, Ananthanarayanan B, Peters D, Tirrell M. Thermodynamic and kinetic stability of DSPE-PEG (2000) micelles in the presence of bovine serum albumin. J Phys Chem B. 2010;114(39):12632–40.
39. Lim SB, Rubinstein I, Sadikot RT, Artwohl JE, Onyüksel H. A novel peptide nanomedicine against acute lung injury: GLP-1 in phospholipid micelles. Pharm Res. 2011;28(3):662–72.
40. Lim SB, Rubinstein I, Onyüksel H. Freeze drying of peptide drugs self-associated with long-circulating, biocompatible and biodegradable sterically stabilized phospholipid nanomicelles. Int J Pharm. 2008;356(1–2):345–50.
41. Jiskoot W, Randolph TW, Volkin DB, Middaugh CR, Schöneich C, Winter G, Friess W, Crommelin DJ, Carpenter JF. Protein instability and immunogenicity: Roadblocks to clinical application of injectable protein delivery systems for sustained release. J Pharm Sci. 2011 in press doi:10.1002/jps.23018.